7-Hydroxyquinoline·(NH$_3$)$_3$: A Model for Excited State H-Atom Transfer Along an Ammonia Wire

Christian Tanner*, Carine Manca, and Samuel Leutwyler

Abstract: The 7-hydroxyquinoline·(NH$_3$)$_3$ cluster has been used as a model to study excited state H-atom transfer along a hydrogen-bonded NH$_3$···NH$_3$···NH$_3$ wire. Excitation of the supersonically cooled cluster to its vibrationless S$_1$ state produces no reaction, whereas excitation of ammonia-wire vibrations induces fluorescence of the excited 7-ketoquinoline·(NH$_3$)$_3$ cluster, revealing the excited state *enol → keto* tautomerization. This reaction is assumed to occur *via* successive H transfers along the ammonia wire in a Grotthus-like process. *Ab initio* calculations of the reaction path show that proton and electron movement along the wire are closely coupled. The rate-controlling S$_1$ state barriers arise from crossing of a $\pi\pi^*$ and a Rydberg-type $\pi\sigma^*$ electronic excited state.

Keywords: Ammonia wire · CIS and CASSCF calculations · Excited state · Hydrogen transfer · Molecular beam

Proton and hydrogen transfer are among the fundamental and best-studied reactions in biology, especially proton transport through membrane ion channels ('proton wires'). Many transmembrane proteins create, control or utilize proton gradients across biological membranes. An example of a so-called 'proton pump' is the photosynthetic reaction center of *Rhodobacter sphaeroides*, which contains a chain of water molecules [1]. Direct experimental observation of the motion of protons along a wire is difficult, because of the short times, microscopic length scales, and solvent fluctuations involved. Thus we focus on simple model systems in order to understand the most basic aspects of proton conduction along hydrogen-bonded wires.

7-Hydroxyquinoline (7HQ) is an aromatic molecule which combines an O–H group as H donor with a quinolinic N acceptor site (Fig. 1a). This molecule is employed as a framework for a hydrogen-bonded wire consisting of three NH$_3$ molecules, the two hydrogen bonding sites being spaced far enough apart to stretch the wire. A different way of looking at the proton transfer process is that the *enol → keto* tautomerization of 7-hydroxyquinoline is mediated by the wire (the keto form is shown in Fig. 1b). Our recent laser spectroscopic experiments on jet-cooled ammonia clusters 7HQ·(NH$_3$)$_n$ have allowed size-dependent studies on the proton transfer process and we have shown that for n = 5 or 6, ground-state proton transfer with formation of zwitterions occurs [2][3]. DFT calculations predict Grotthus-type proton transfer steps along the wire [2]. For the n = 3 cluster, no reaction has been found in the ground state. Indeed, *ab initio* calculations predict the enol form to be 36 kJ mol^{-1} more stable than the keto in the gas phase; the latter is not observed in our supersonic molecular beam experiments at 5 K.

In the S$_1$ state, the keto form is predicted to be 46 kJ mol^{-1} more stable than the enol. The SCF and CIS geometry optimizations in the ground and the excited state allows the estimation of the geometry changes upon S$_1$ ← S$_0$ excitation: All four hydrogen bonds contract, as indicated in Fig. 1a, by –0.03 to –0.08 Å, the larger decreases occurring at the ends of the wire. In parallel, the intramolecular O–H bond is predicted to lengthen by +0.01 Å. These geometric changes upon excitation of 7HQ are intuitively expected to favor the *enol → keto* reaction.

The S$_1$ ← S$_0$ two-color resonant 2-photon ionization (2C-R2PI) spectrum of 7HQ·(NH$_3$)$_3$ is shown in Fig. 2a: it is mainly composed of sharp bands (FWHM of 1–2 cm^{-1}) in the range 28800–29000 cm^{-1}. The most intense band at 28798.4 cm^{-1} is assigned to the electronic origin. The band at +13 cm^{-1} is an ammonia wire bending mode and the stronger bands in the range +125 to +200 cm^{-1} correspond to ammonia wire stretching vibrations; for more details, see [4].

The UV-UV depletion spectrum shown in Fig. 2b is obtained by scanning a hole-burning laser over the same spectral region, 300 ns before the 2C-R2PI measurement, thereby depopulating the vibrational ground state. The resulting UV-UV depletion spectrum shows the same components as the 2C-R2PI spectrum from the origin up to 200 cm^{-1}. Contrary to the 2C-R2PI spectrum, it exhibits further vibronic bands far above 200 cm^{-1}. Complementary measurements of UV fluorescence (not shown here) present a similar falloff at ~ 200 cm^{-1} above the electronic origin. The loss of both the 2C-R2PI and UV fluorescence signals reveals the loss of the excited state enol 7HQ*·(NH$_3$)$_3$ cluster population and prove the onset of a fast process at ~200 cm^{-1} excess energy in the S$_1$ state.

Concurrent to the loss of the UV fluorescence of 7HQ*·(NH$_3$)$_3$, we observe an

Correspondence: C. Tanner
Universität Bern
Department für Chemie und Biochemie
Freiestrasse 3
CH-3000 Bern 9
Tel.: +41 31 631 42 38
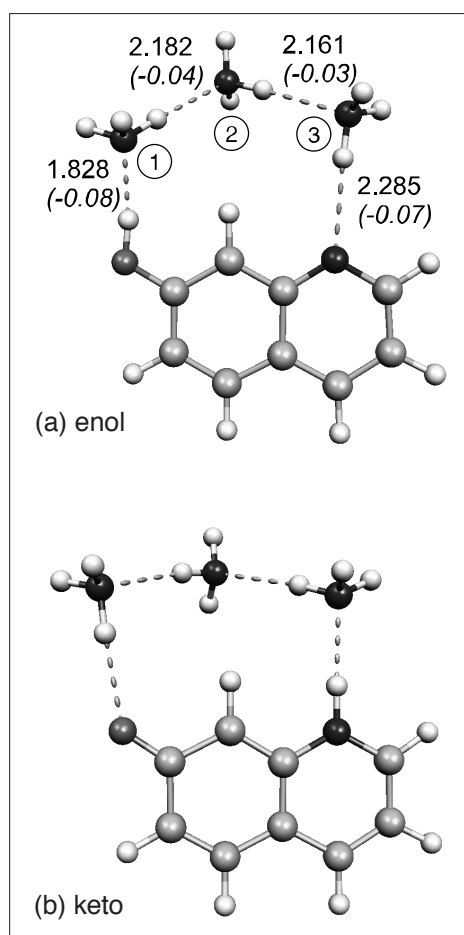Fax: +41 31 631 39 94
E-Mail: christian.tanner@iac.unibe.ch

Fig. 1. Calculated stable structures of the enol (a) and the keto (b) tautomeric forms of the 7-hydroxyquinoline 7HQ·(NH$_3$)$_3$ cluster. For the enol form, hydrogen bond lengths between H and heavy atom in the ground state are indicated in Å, changes upon excitation are given in parentheses.

increase in yellow fluorescence. Such fluorescence has already been observed in bulk protic solvents and has been assigned to the S$_1$ state 7-ketoquinoline (7KQ*) tautomer [5]. Fluorescence excitation spectra (scanning the excitation laser and monitoring the maximum of the yellow fluorescence at 18360 cm^{-1}, Fig. 2c) exhibit the same characteristic vibronic band pattern of 7HQ·(NH$_3$)$_3$ as in the UV-UV depletion, starting from the two highest vibronic bands observed in the 2C-R2PI spectrum, 200 cm^{-1} above the origin (the remaining fluorescence background arises from larger 7HQ·(NH$_3$)$_n$ clusters). In other words, the excitation of 7HQ·(NH$_3$)$_3$ clusters ≥ 200 cm^{-1} above the electronic origin leads to formation and fluorescence emission of the 7KQ*·(NH$_3$)$_3$ cluster.

We used CIS and CASSCF excited state calculations in order to interpret the experiments and propose a mechanism. We assume that the excited state *enol → keto* tautomerization observed involves H$^+$ or H translocation along the (NH$_3$)$_3$ wire to the quinolinic N atom, in a Grotthus-type reaction [6]. The upper part of Fig. 3 shows the

schematic S$_1$ potential connecting all the fully optimized CIS stationary structures obtained. The ground-state enol form has been taken as reference for these calculations and the excited-state potential has been arbitrarily offset to match the experimental value of the electronic origin. We have found three minima between the enol and the keto form: these correspond to the H-atom transferred intermediates denoted HT1, HT2, and HT3 respectively. These are separated by four transition states labeled TS$_{E/1}$, TS$_{1/2}$, TS$_{2/3}$, and TS$_{3/K}$. Fig. 4 shows the first reaction step between enol and HT1, involving an H transfer from the hydroxyl group of 7HQ to the first ammonia molecule. The three other steps can be obtained by the corresponding H transfer through the ammonia wire to the quinolinic N.

Further CASSCF calculations were performed with the cluster constrained to C_s symmetry to clarify the key points of the reaction. The S$_1$ and S$_2$ potentials obtained with these calculations are schematically shown in Fig. 3 (dotted and dashed lines). The calculations predict that the S$_1$ ← S$_0$ excitation occurs dominantly from the highest occupied π molecular orbital on 7HQ. The enol S$_1$ state is a ππ* (A') excita-

tion localized on 7HQ, whereas the S$_2$ state is mainly a πσ* (A'') Rydberg-type excitation. Due to different spatial symmetry, these states can cross along the reaction path between the enol and the HT1 forms and create a conical intersection. In nonplanar geometries, such an intersection is forbidden, leading to repulsion of the two states in an adiabatic description. The barrier at TS$_{E/1}$ of the CIS calculations originates from the crossing of the ππ* and πσ* states, indicating a qualitative change of the excited state character. The CIS calculated electronic barrier height is 3720 cm^{-1} (44.5 kJ mol^{-1}) which is probably too high since the CIS method is known to typically overestimate such barriers [7]. The *enol → HT1* step is predicted to be exoergic by about 2600 cm^{-1} (31.1 kJ mol^{-1}), which provides the driving force of the reaction. The last barrier at TS$_{3/K}$ in CIS calculations originates from a reverse crossing between the πσ* and ππ* states as diagnosed in the CASSCF calculations, leading to the ππ* excited 7KQ*·(NH$_3$)$_3$ tautomer. According to the CIS calculation, the HT1, HT2, HT3, and 7KQ forms lie close in energy; once the system passes through the TS$_{E/1}$ barrier, the two subsequent barriers are surmounted. The last barrier TS$_{3/K}$ between the HT3 and

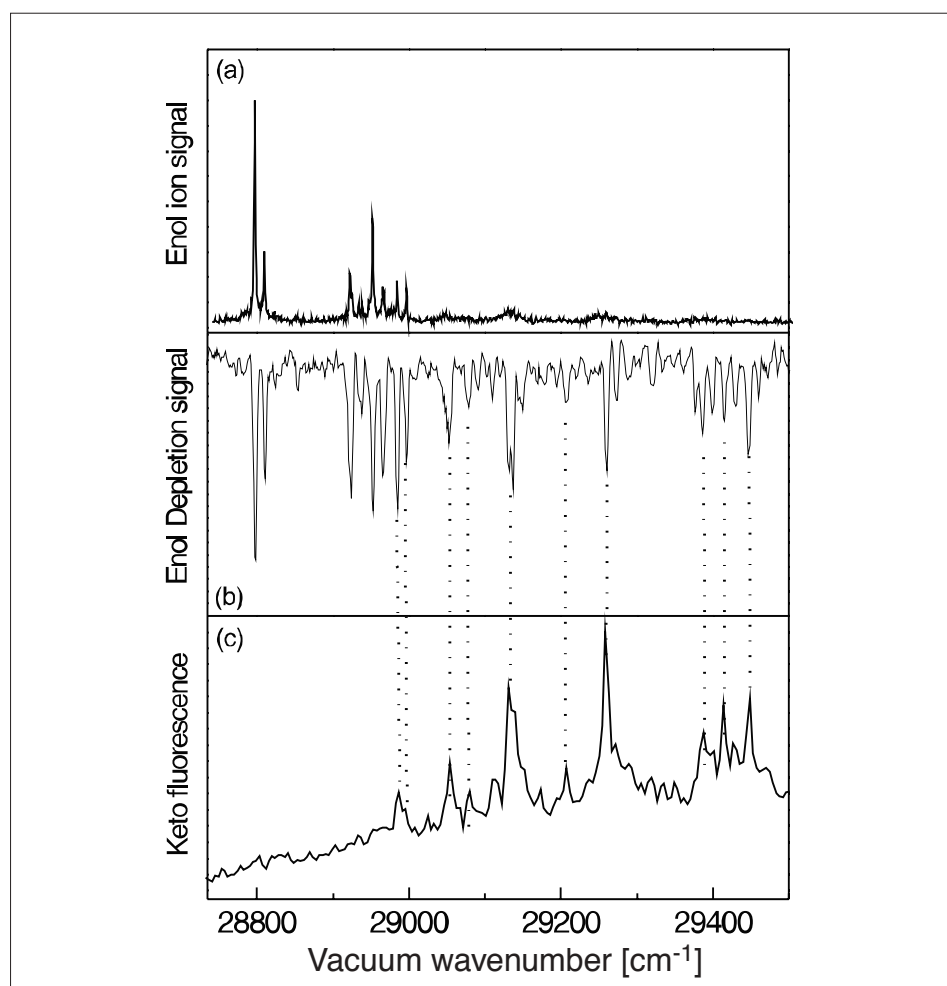Fig 2. a: 2-Color Resonant 2-Photon Ionization spectrum of 7HQ·(NH$_3$)$_3$. b: UV-UV depletion spectrum of 7HQ·(NH$_3$)$_3$. c: Excitation fluorescence of 7HQ·(NH$_3$)$_3$ at 18360 cm^{-1}.
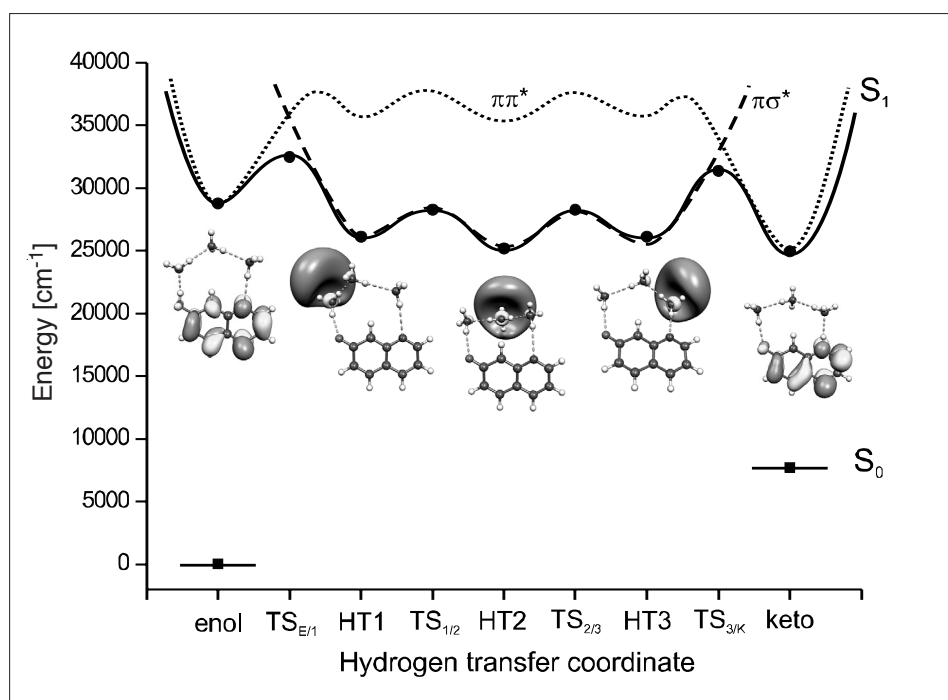
Fig 3. Excited state (S_1) *enol* → *keto* conversion pathways of 7HQ·(NH$_3$)$_3$. The full line indicates the CIS potential. The dotted and dashed lines schematically indicate the $\pi\pi^*$ and $\pi\sigma^*$ states calculated with the CASSCF method. The energies of the enol and the keto form in the ground state (S_0) are also indicated. The unoccupied molecular orbital that contributes dominantly to the S_1 state wave function is shown for the enol, the keto and the three intermediate minima.
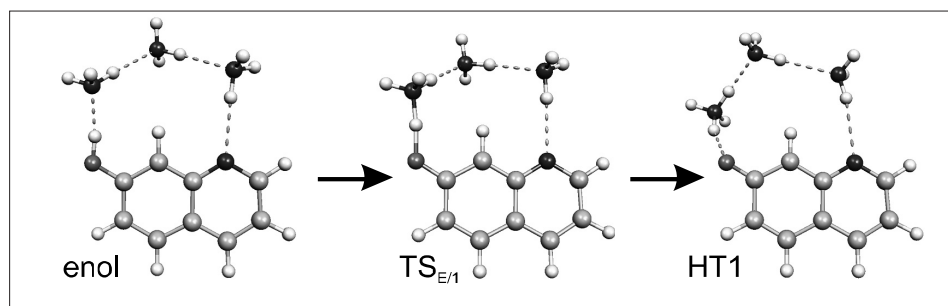

Fig 4. The reactant, transition state and product structures for the first step of the proposed H-atom transfer reaction between the enol and the HT1 form, TS$_{E/1}$ being the transition state.

7KQ forms is calculated to be nearly as high as TS$_{E/1}$. The $S_1 \leftarrow S_0$ energy difference for 7KQ after S_1 state translation (see above) is predicted to be 18,020 cm^{-1}, in agreement with experimental fluorescence maximum at 18,360 cm^{-1}.

The configuration contributing dominantly to the excited wave function involves promotion of an electron from the highest occupied π orbital of 7HQ. The change in character of the electron-accepting antibonding orbital has already been detailed elsewhere [8]. Briefly, for the enol, this is the antibonding π^* orbital of 7HQ, whereas for HT1 it is an antibonding σ^* orbital on the newly generated NH$_4$ moiety (Fig. 3). A transfer of 0.9 electron from the 7HQ moiety to NH$_3$ (1) occurs simultaneously with this change of excited-state character: the proton transfer becomes a H atom transfer in the vicinity of TS$_{E/1}$. The lowest excited state retains the σ^* character along the translocation coordinate up to TS$_{3/K}$ and the

σ^* orbital accompanies the H atom (Fig. 3). A reverse $\sigma^* \rightarrow \pi^*$ state switching occurs near TS$_{3/K}$; the 7KQ orbital is a π^* orbital similar to that of the enol.

We emphasize the correlation between the $\pi^* \rightarrow \sigma^* \rightarrow \pi^*$ crossovers and the changes of oscillator strength for the $S_1 \rightarrow S_0$ transition: According to C_s symmetry selection rules, fluorescence is allowed from the $\pi\pi^*$ but forbidden from the $\pi\sigma^*$ state and this selection rule holds approximately also for non C_s geometry here: The calculated $S_1 \rightarrow S_0$ oscillator strength for 7HQ and 7KQ like states are f = 0.193 and 0.294 respectively, whereas for HT1 to HT3 states they are f = 0.001 to 0.004. This difference explains why the HT1, HT2 and HT3 forms have much longer radiative lifetimes and why no fluorescence is observed from these intermediates in our experiments.

The role of low-lying $\pi\sigma^*$ Rydberg-type electronic states for excited state hydrogen transfer of heteroaromatic mole-

cules has been studied for phenol, indole, 1-naphthol·(NH$_3$)$_n$ and phenol·(NH$_3$)$_n$ clusters [7][9]. For all these systems, the lowest $\pi\sigma^*$ excited states are *dissociative* along the N–H or O–H bond stretching coordinates. Concerning the 7HQ·(NH$_3$)$_3$, it is worth noting that the $\pi\sigma^*$ state does *not* lead to cluster dissociation but to H atom transfers from the O-H group of 7HQ along the ammonia wire.

Summarizing, we have shown that H atom transfer can be induced along the ammonia wire connected to 7-hydroxyquinoline in the S_1 excited state. Additional excitation of S_1 state ammonia wire vibrations is necessary to activate the reaction (2.5 kJ mol^{-1} experimentally). *Ab initio* calculations predict a crossing of $\pi\pi^*$ and $\pi\sigma^*$ potential energy curves along the H atom transfer coordinate that creates an initial barrier of ~44 kJ mol^{-1}. At least the first reaction step involves quantum tunneling from the ground state of the O–H mode. It is exothermic by about 30 kJ mol^{-1}, which provides the driving force for the subsequent reaction steps.

[1] U. Ermler, G. Fritzsch, S. Buchanan, H. Michel, *Structure* **1994**, *2*, 925.

[2] M. Meuwly, A Bach, S. Leutwyler, *J. Am. Chem. Soc*. **2001**, *123*, 11446.

[3] A. Bach, C. Tanner, C. Manca, H.-M. Frey, S. Leutwyler, *J. Chem. Phys.* **2003**, *119*, 5933.

[4] C. Manca, C. Tanner, S. Coussan, A. Bach, S. Leutwyler, *J. Chem. Phys.*, submitted.

[5] S.F. Mason, J. Philip, B.E. Smith, *J. Chem. Soc. A*. **1968**, 3051; S. Schulman, Q. Fernando, *Tetrahedron* **1968**, *24*, 1777; K. Tokumura, M. Ioth, *J. Phys. Chem.* **1984**, *88*, 3921; E. Bardez, *Israel J. Chemistry* **1999**, *39*, 319.

[6] D. Borgis, J. Hynes, *Chem. Phys.* **1993**, *170*, 315; N. Agmon, *Chem. Phys. Lett*. **1995**, *244*, 456; D. Marx. M.E. Tuckerman, J. Hutter, M. Parrinello, *Nature* **1999**, *397*, 601; P.L. Geissler, C. Dellago, D. Chandler, J. Hutter, M. Parrinello, *Science* **2001**, *291*, 2121; D. Lu, G.A. Voth, *J. Am. Chem. Soc.* **1998**, *120*, 4006; R. Vuilleumier, D. Borgis, *J. Phys. Chem. B* **1998**, *102*, 4261; H.S. Mei, M.E. Tuckerman, D.E. Sagnella, M.L. Klein, *J. Phys. Chem. B* **1998**, *102*, 10446.

[7] A.L. Sobolewski, W. Domcke, *Phys. Chem. Chem. Phys.* **1999**, *1*, 3065; A.L. Sobolewski, W. Domcke, *J. Chem. Phys. A* **2001**, *105*, 9275; A.L. Sobolewski, W. Domcke, C. Dedonder-Lardeux, C. Jouvet, *Phys. Chem. Chem. Phys.* **2002**, *4*, 1093.

[8] C. Tanner, C. Manca, S. Leutwyler, *Science* **2003**, *302* , 1736.

[9] A.L. Sobolewski, W. Domcke, *J. Chem. Phys. A* **1999**, *103*, 4494; O. David, C. Dedonder-Lardeux, C. Jouvet, *Int. Rev. Phys. Chem.* **2002**, *21*, 499.